

# Prognostics of systemic malignancy ICD-O topography and morphology types on brain metastases: an NCDB time-to-event cohort

Georgios Alexopoulos (✉ [alexopoulos\\_george@hotmail.com](mailto:alexopoulos_george@hotmail.com))

Saint Louis University Hospital

Justin Zhang

Saint Louis University

Ioannis Karampelas

Banner Health

Mayur Patel

Saint Louis University

Philippe Mercier

Saint Louis University Hospital

---

## Research Article

**Keywords:** brain metastases, cerebral metastases, brain metastasis, metastatic disease, topography, morphology, systemic malignancy

**Posted Date:** April 18th, 2022

**DOI:** <https://doi.org/10.21203/rs.3.rs-1559460/v1>

**License:**  This work is licensed under a Creative Commons Attribution 4.0 International License.

[Read Full License](#)

---

# Abstract

**Purpose:** The site and histology of primary cancer are known predictors of progression to brain metastases(BM). We investigated the combinational interactions of ICD-O primary topography and morphology types on the survival of BM after adjusting for relevant clinical and demographic prognostic factors.

**Methods:** The cohort included all adult patients with BM at diagnosis of an invasive malignancy in the National Cancer Database(2010-2018). The sample consisted of 180,150 entries out of 14,279,749 cancer patients screened. A survival analysis of the topography- and histology- specific time to death was performed. Multivariate Cox regression revealed violations of the proportional hazard assumption for multiple covariates. Parametric models using a log-logistic distribution best described the population survival pattern.

**Results:** The primary topography “prostate” and morphology “choriocarcinoma” provided the strongest survival benefit among ICD-O types, while BM from prostate demonstrated a 14-month median overall increase in survival probability. Favorable prognostics were BM from breast, bone/joints, and testis; also, the morphologies of carcinoid tumor, mature B-cell lymphoma, and papillary adenocarcinoma. Poor prognostics were BM from gastrointestinal(liver, biliary tree, pancreas, gallbladder) and gynecologic malignancies. All morphologies of spindle cell carcinoma, hemangiosarcoma, undifferentiated carcinoma, Ewing sarcoma, pseudosarcomatous carcinoma, renal cell carcinoma/sarcomatoid, signet ring cell carcinoma, spindle cell sarcoma, and squamous cell carcinoma/spindle cell were associated with poor survival.

**Conclusions:** This is the largest cohort providing an unbiased estimate of the adjusted ICD-O topography and morphology effect sizes. The results can be summarized as a booklet for prognostic classification of disease in patients with BM secondary to systemic malignancy.

## Key Points

- The largest cohort of adult patients with synchronous brain metastases secondary to an invasive malignancy.
- Booklet for prognostic classification of brain metastatic disease.

## Importance Of The Study

This study is the largest cohort of adult patients with synchronous brain metastases secondary to an invasive malignancy, as these reported in the National Cancer Database (NCDB). We investigate the combinational interactions between primary topography and morphology types, based on the International Classification for Diseases in Oncology. The results can be summarized as a booklet for prognostic classification of brain metastatic disease, and the study can become a valuable and updated companion to the graded prognostic assessment tool for clinical trial design.

# Introduction

Brain metastases (BM) are the most frequent type of CNS tumor in adults.<sup>1-3</sup> Population-based studies report the incidence of metastatic brain cancer ranging from 8.3 to 14.3 per 100 000.<sup>2-4</sup> Other authors support that up to one-fifth of adult cancer tumors will eventually metastasize to the brain.<sup>3,6,7</sup> The exact incidence of BM remains unknown, while the reported rates in the literature are estimates at best.<sup>1-7</sup> Despite being a major source of morbidity and mortality, large-scale cohorts examining the prognostics of BMs are lacking.<sup>1-6</sup> Most of the survival data that do exist regarding patients with BM are based on studies decades old having several methodological limitations.<sup>3,5,6</sup> These studies are scarce, with only four population-based reports on BMs having been published recently.<sup>2-6</sup> Better understanding of the epidemiology and prognostics of BM will help identify individuals who are at greatest risk and guide clinicians in selecting patients who are most likely to benefit from surveillance and prophylaxis.<sup>1-6</sup>

The natural history of progression to BM varies according to site (topography) and histology (morphology) of the systemic malignancy.<sup>6-11</sup> Lung cancer, breast cancer, melanoma and colorectal cancer are the most frequent to develop BM, and account for 67%-80% of all BM.<sup>2,5,7,10</sup> A tumor topography-related study in the Detroit metropolitan area from 1973 to 2001 reported that the incidence of BM was highest for lung (19.9%), followed by melanoma (6.9%), renal (6.5%), and breast (5.1%) cancers.<sup>12</sup> The overall prognosis of BM depends on the primary topography, histology, clinical, and treatment factors.<sup>8,10-13</sup> Despite these key reports, no large cohorts have established a time-to-event analysis implementing the combined effect of primary malignancy topography and morphology types on patient prognosis. In our study, we utilize data from the National Cancer Database of the American Cancer Society,<sup>14</sup> one of the largest hospital-based registries worldwide to identify the prognostics of various systemic malignancy topography and morphology types on BM, based upon the revised guidelines for International Classification of Diseases for Oncology (ICD-O).<sup>9</sup> Through a comprehensive survival analysis workflow, our study is the first to report the combinational interactions of ICD-O primary topography and morphology types on the survival of patients with BM after adjusting for multiple relevant clinical and demographic factors.

## Methodology

### Data and study population

Data were extracted from the National Cancer Database (NCDB). The NCDB is a joint program of the Commission on Cancer and the American Cancer Society including nationwide data from more than 1,500 Commission-accredited cancer facilities in the United States and Puerto Rico.<sup>14</sup> The entire NCDB adult registry [ages: 18-90+] from year 2010 to 2018 was filtered by “CS\_METS\_DX\_BRAIN” == ‘YES’ (Item #: 2852; 2010-2015) OR “METS\_AT\_DX\_BRAIN” == ‘YES’ (Item #: 1113; 2016-2018). All patients with BM at diagnosis of an invasive malignancy originating outside the CNS were included. Patients with non-invasive neoplasms were not included in this study. To control for Type S (sign) and Type M (magnitude)

errors,<sup>15</sup> we retroactively performed a design analysis and found ICD-O types with small-sample brain metastases ( $N < 42$ ) resulting in misleading statistically significant estimates. After removing the noisy small-sample sites of origin (Items #: 2852 OR 1113 == 'YES' < 42 patients with BM per topography), we identified a total of 180,325 subjects with BM out of 14,279,749 cancer patients screened (Table1). Based on the ICD-O-3 topographies,<sup>9</sup> 175 patients with BM from extra-nodal NHLs and reported codes C71.0 to C72.9 were further excluded, given CNS was identified as the site of origin. The final sample consisted of 180,150 unique observations of cancer patients with BM and 91 variables were extracted from each record including the primary cancer type or topography, tumor histology or morphology, and the detailed anatomic site of origin (supplement). No duplicate patient ID entries were identified. All topography and morphology codes were reported according to ICD-O-3 (first revision).<sup>9</sup>

## Survival analysis

The cohort included all cancer patients with BM at diagnosis as reported in the NCDB between the years 2010 and 2018. The target events for this study were the origin site-specific time to death from the time of diagnosis, or death attributable to primary topography, and the histology-specific time to death, or death attributable to morphology. The time origin was set as the point at which a subject was diagnosed with BM, and the time scale was the patient survival in months as reported in the NCDB. We had no reason to suspect informative censoring in a large multicenter database such as the NCDB. The events constituted independent random samples and the subpopulation was screened for duplicate patient entries. Non-parametric analysis was initially utilized to generate unbiased descriptive estimates, in conjunction with semi-parametric or parametric tests whenever necessary. Rank-based tests, such as the log-rank test, were used to statistically test the difference between the Kaplan-Meier survival curves. The semi-parametric Cox Proportional model was used for univariate and multiple regression analysis to estimate the hazard ratios. The proportional hazards (PH) assumption necessitates a constant relationship between the outcome and the covariates over time, and therefore, it is vital for interpretation of the Cox regression. The PH assumption for each predictor in the Cox models was tested calculating the scaled Schoenfeld residuals over time for factors, and the Martingale residuals for continuous variables. Parametric survival models, or accelerated failure time models (AFT), are alternatives to Cox regression, and one of the few available substitutes when the PH assumption is frankly violated.<sup>16</sup> Parametric survival analysis in our study included the exponential, Weibull, Gompertz, gamma, generalized gamma, lognormal and log-logistic distributions to identify the best survival population pattern to fit our data. Feature selection was performed using stepwise AIC backward regression by starting from a maximal model including all candidate predictor variables in the study. We used AIC and likelihood ratio tests to assess for relative model goodness of fit followed by the  $\log(-\log(S(t)))$  plots to check for model validity and evaluate the pattern of survival estimates against time. Here, we report the multiple regression analysis results of the best parametric model in conjunction with those extracted from Cox regression.

## Software

All analyses were implemented using the R statistical software, version 4.1.2. Non-parametric and semiparametric survival approaches were completed using the “survival” and “survminer” packages. Feature selection was performed using “stepAIC” in MASS. Parametric distribution model fit was performed using the “flexsurv” package, while Kaplan-Meier estimates and the respective effect sizes from parametric bootstrap simulation were generated using the “survParamSim” implementation in R.

## Results

### 1) Univariate statistics

#### 1.1 Nonparametric survival analysis

The median topography-specific survival time in cancer patients with BM, or the time when the survival probability,  $S(t)$ , decreased by 50%, was 17.9 months in tumors originating from the testis (95%CI[15.2,26.9]; $p < 0.0001$ ). Patients with BM from nodal NHLs had a median survival of 13.6 months (95%CI[10.6,20.3]; $p < 0.0001$ ), prostate metastases reached a  $S(t)$  of 15.8 months (95%CI[12.7,18.3]; $p < 0.0001$ ) while patients with BM originating from breast had a  $S(t)$  of 10.7 months (95%CI[10.2,11.5]; $p < 0.0001$ ), as shown in Figure 1. The topographies with the lowest median survival times were lung(other type),  $S(t) = 1.8$  months (95%CI[1.74,1.84]; $p < 0.0001$ ), pancreas,  $S(t) = 2.3$  months (95%CI[2.20,2.60]; $p < 0.0001$ ), urinary tracts,  $S(t) = 2.4$  months (95%CI[1.87,3.30]; $p < 0.0001$ ) and liver,  $S(t) = 2.6$  months (95%CI[2.10,3.06]; $p < 0.0001$ ). The Kaplan-Meier estimates of systemic malignancy topography on patient survival are demonstrated in Figures 1 and 2. When comparing the most common origin sites of BM, as previously reported in the literature,<sup>1-6</sup> there is a continuous survival advantage among patients with prostate cancer by a 14-month median overall increase in the survival probability.

The median morphology-specific survival time was highest, or 18.4 months (95%CI[13.2,25.4];  $p < 0.0001$ ), in patients with infiltrating duct and lobular carcinoma. BM originating from acinar cell carcinomas had a median survival of 16.3 months (95%CI[12.6,18.6]; $p < 0.0001$ ), while patients with malignant struma ovarii metastatic to the brain achieved an  $S(t)$  of 15.2 months (95%CI[13.7,19.3]; $p < 0.0001$ ). BM originating from malignant neoplasms (ICD-O-3, #8000/3) had the lowest median survival of 1.3 months (95%CI[1.25,1.38]; $p < 0.0001$ ), followed by spindle cell carcinomas not otherwise specified,  $S(t) = 2.4$  months (95%CI[2.10,3.61]; $p < 0.0001$ ) and hepatocellular carcinomas,  $S(t) = 2.7$  months (95%CI[2.14,3.19]; $p < 0.0001$ ).

#### 1.2 Cox regression analysis

The regression beta coefficients along with the hazard ratios (HR) and variable significance based on the topography and morphology of systemic disease were calculated for the variables of interest. Each predictor was assessed through separate Cox regression analysis followed by stratified Cox. The PH assumption was frankly violated for multiple covariates in the NCDB population, and proportionality was unable to be achieved after multiple stratification attempts (supplement).

All the following primary topography types: pancreas, liver, biliary, urinary tracts, lung(other) were associated with poorer survival in patients with BM (Figure3). Tumors originating from testis, nodal NHL, extra-nodal NHL, and prostate were associated with improved survival. Furthermore, BM originating from extra-nodal NHLs reduced the hazard factor by 32% (HR= 0.68, 95%CI[0.52,0.88];p < 0.0001), followed by BM from testis with a HR decrease by 31% (HR= 0.69, 95%CI[0.59,0.81];p < 0.0001) when compared with metastases from prostate cancer (Figure3).

In the univariate Cox regression, choriocarcinomas showed the best overall survival benefit among all morphology groups. Spindle cell carcinomas not otherwise specified (HR= 9.21, 95%CI[0.39,0.75]; p < 0.0001), hepatocellular carcinomas (HR= 8.21, 95%CI[4.72,14.28]; p < 0.0001), and malignant neoplasms (ICD-O-3 code #8000/3) were poor morphology prognostics in cancer patients with BM (supplement).

## 2) Multiple regression analysis

### 2.1 Feature selection

Feature selection started from a full, or saturated, survival model including all 91 variables in the study (supplement). The optimal regression model was the one that minimized the AIC using stepwise backward elimination. The best model to describe the data was the one featuring the seventeen covariates demonstrated in Table2.

### 2.2 Semiparametric vs parametric survival analysis

We fit a Cox model using all the significant covariates from feature selection. The HRs for each respective covariate can be seen in the supplement. The Schoenfeld residuals test was significant for multiple covariates in the model. The non-proportionality was further supported by graphical diagnostics given the  $\log(-\log(S(t)))$  plots did not demonstrate any parallelism (supplement). We were unable to correct for nonproportionality in the Cox model after multiple stratification attempts. We concluded that the estimates derived from utilizing Cox regression in the study should not be generalized, as semiparametric regression led to incorrect inferences. AFT models are especially important under such circumstances, given their parametric distribution for the survival times AFT models can make statistical inference accurate and lead to a proper model fitting.<sup>16</sup>

### 2.3 Parametric model fit and results

Relative to other parametric distribution results, the log-logistic distribution achieved the lowest AIC and likelihood ratio tests indicating a more parsimonious model able to better describe the NCDB population survival pattern (Figure4). The log-logistic distribution has a non-monotonic arc-shaped decreasing hazard rate. The absolute parametric model goodness of fit for validity was assessed through Q-Q graphical plots, which demonstrated linearity in a function of time for the loglogistic model. Next, we fit a loglogistic AFT model using all the significant variables from feature selection.

#### 2.3.1 Topography and morphology

We identified the topography “prostate” as the best overall prognostic among sites of origin in patients with BM (Table2). The median life expectancy for metastatic liver cancer was 10.1 times less (PO= 10.1, 95%CI[6.14,16.5];p < 0.0001) that of BM from prostate. BM from the biliary tree (PO= 8.14, 95%CI[5.37,12.3];p < 0.0001), pancreas (PO= 7.52, 95%CI[6.12,9.24];p < 0.0001), and gallbladder (PO= 7.17, 95%CI[4.67,11.0];p < 0.0001) were associated with poor survival. Similarly, ovarian (PO= 8.48,95%CI[6.09,11.8];p< 0.0001), uterine (PO= 8.49, 95%CI[6.61,10.9];p < 0.0001), and cervical (PO= 8.68, 95%CI[6.65,11.3];p < 0.0001) cancers were poor prognostics. In contrast, patients with BM originating from breast (PO= 3.44, 95%CI[2.81,4.22]; p < 0.0001), bone/joints (PO= 3.22, 95%CI[1.63,6.34];p < 0.0001), and testis (PO= 3.27, 95%CI[1.65,6.45];p < 0.0001) had an improved overall survival second only to that of prostate cancer.

The histology “choriocarcinoma” has been reported as a potential favorable prognostic in BM,<sup>17</sup> therefore it was utilized as the morphology reference group in the model. Similarly, the histopathology choriocarcinoma was among the best overall morphology prognostics along with mature B-cell lymphomas (Table2). Other good prognostics were carcinoid tumor (PO= 2.72, 95%CI[1.11,6.68];p < 0.0001) and papillary adenocarcinoma (PO= 4.12, 95%CI[1.77,9.58];p < 0.0001). The combined morphology category cystic mucinous and serous carcinomas (ICD-O-3 codes #844-849) was associated with increased survival. In contrast, the median life expectancy for metastatic spindle cell carcinoma was 19.4 times less (PO= 19.4, 95%CI[7.77,48.4];p < 0.0001) that of choriocarcinoma. Hemangiosarcoma was also among the worse prognostics (PO= 18.6, 95%CI[7.3,47.2];p < 0.0001). The remaining morphology groups associated with poor survival were carcinoma undifferentiated (PO= 14.6, 95%CI[5.88,36.4];p < 0.0001), Ewing sarcoma (PO= 14.0, 95%CI[4.55,43.3];p < 0.0001), malignant neoplasm (PO= 15.9, 95%CI[6.91,36.7];p < 0.0001), pseudosarcomatous carcinoma (PO= 13.8, 95%CI[5.92,32.2];p < 0.0001), renal cell carcinoma/sarcomatoid (PO= 14.0, 95%CI[5.81,33.9];p < 0.0001), signet ring cell carcinoma (PO= 12.2, 95%CI[5.22,28.6];p < 0.0001), spindle cell sarcoma (PO= 14.5, 95%CI[5.34,39.2];p < 0.0001) and squamous cell carcinoma from spindle cells (PO= 13.5, 95%CI[4.97,36.5];p < 0.0001). Tumors in the combined morphology category osseous and chondromatous neoplasms (ICD-O-3 codes #918-924) were poor prognostics (Table2).

### *2.3.2 Demographics and patient specific factors*

The median survival for males was 1.24 times less that of females when adjusting for other covariates in the model (PO= 1.24, 95%CI[1.22,1.27];p < 0.0001). Increasing patient age, White race, and American Indians or Eskimos were bad prognostics (Table2). Asian race demonstrated a protective effect as the survival was accelerated by a factor of 1.3 (AF= 1.3, 95%CI[1.25,1.36];p < 0.0001) when compared to Black patients. Increasing Charlson-Deyo comorbidity score (CDScore) was associated with poor survival, while patients with a CDscore of 3 had the worse overall prognosis (PO= 1.52, 95%CI[1.45,1.59];p < 0.0001) among other CDscore groups. The median patient income and level of education did not achieve significance in the model. In patients with coexisting liver metastatic disease the median life expectancy was decreased by half (PO= 1.99, 95%CI[1.95,2.04];p < 0.0001).

### 2.3.3 Type of treatment

Patients with BM who underwent surgery of the primary site with no residual tumor margins had 2.07 times increased overall survival (AF= 2.07, 95%CI[1.72,2.49];p < 0.0001). Failure of administering chemotherapy, despite being part of first course treatment, decreased the median survival by 4.31 (PO= 4.31, 95%CI[4.13,4.49];p < 0.0001). Similarly, no administration of radiotherapy (PO= 1.59, 95%CI[1.5,1.68];p < 0.0001), immunotherapy (PO= 2.01, 95%CI[1.66,2.44]; p < 0.0001) and hormone therapy (PO= 2.53, 95%CI[2.34,2.74];p < 0.0001) were all associated with shorter survival times.

## Discussion

BM continue to foreshadow a poor prognosis for all cancer patients.<sup>1-6</sup> In 80% of the cases, BM are discovered in a metachronous fashion, but less frequently, BM can be diagnosed at the same time as the systemic malignancy (synchronous diagnosis).<sup>5-8</sup> The sources of BM(in descending order) are cancers of the lung, breast, skin, kidney, and gastrointestinal (GI) tract.<sup>2,5,7,10</sup> In the NCDB, all lung cancer morphology types demonstrated an increased frequency for synchronous BM with an approximately 9% of small cell lung cancer (SCLC) patients presenting with BM at the diagnosis of systemic disease (Table 1). Previous studies have also reported 10% of SCLC patients overall presenting with synchronous BM.<sup>1-4,21</sup> Furthermore, GI tract malignancies in the study demonstrated an increased frequency of synchronous BM, especially patients with primary esophageal cancer (1.1%).

The prognosis of BM varies depending on the primary topography, morphology, treatment status, and key patient factors.<sup>1-8</sup> The graded and upgraded prognostic assessments (GPA) remain some of the most valuable prognostic tools for common histologic types of BM.<sup>13,18,19</sup> The Radiation Therapy Oncology Group had previously developed a prognostic classification system for BM patients based on recursive partitioning analysis of performance status, age, and systemic tumor activity.<sup>20</sup> Large-scale studies reporting the combinational interactions of various prognostics on the survival of BM patients are still lacking.<sup>1-8</sup>

Cagney et al utilized population-based data to identify 26,430 patients with synchronous BM and analyzed the incidences of various topographies; the authors reported BM secondary to prostate and breast cancer as having the longest median survival times.<sup>10</sup> We identified prostate cancer and breast cancer providing the strongest survival benefit among other topography types, while further reporting BM originating from bone/joints and testicular cancer as favorable prognostics. Gynecologic and GI malignancies with synchronous BM, especially those originating from liver, pancreas, uterus, cervix, and the ovaries demonstrated the poorest survival in our study. A recent systematic review reported that BM from cervical cancer could reduce longevity independent of overall tumor burden.<sup>22</sup> Our cohort is the first study to calculate the adjusted effect sizes between the various ICD-O topography types and further provide evidence to support such a statement (Table 2). Scant single institution reports have identified patients with BM originating from choriocarcinoma and carcinoid tumors as potential long-term

survivors.<sup>17,23,24</sup> Here, we showed how the histology choriocarcinoma was the most influential among other morphology types, followed by carcinoid tumor and mature B-cell lymphomas (Table 2). Our study is also the first in the literature to identify various spindle cell-derived malignancies as poor prognostics, such as, spindle cell carcinoma, spindle cell sarcoma and squamous cell carcinoma from spindle cells. Choi et al reported the sarcomatoid histology component in BM from renal cell carcinomas(RCC) as a bad prognostic,<sup>25</sup> we further expand the authors' statement to the sarcomatoid component in BM from RCC is a poor predictor of survival among all ICD-O morphologies. BM from GI signet ring cell carcinomas are extremely rare;<sup>26</sup> here we first identified the morphology as a bad prognostic. Pediatric BM from Ewing sarcoma carry a grave prognosis,<sup>27</sup> but adult BM from Ewing sarcoma also demonstrated a poor survival in our study. Favorable demographic factors for enhanced BM survival included female sex, Asian race and lower CDscore (Table 2). Several efficacious therapeutic options were associated with improved survival in our cohort including surgery of the primary site without residual tumor margins, and, whenever part of first course treatment, the administration of radiotherapy, chemotherapy, immunotherapy, and hormone therapy; our findings here are in concordance with previous literature.<sup>1-8</sup>

The accurate and generalizable estimation of effect sizes of the various influential survival predictors in cancer patients with BM is important for clinical trial design. This NCDB study is the largest published cohort, while our multiple regression model also provides an unbiased estimate of the various ICD-O topography and morphology effect sizes by simultaneously adjusting for multiple other known predictors. We provide an important updated companion to the GPA tool which would allow clinicians to estimate survival, individualize treatment, and stratify clinical trials in patients with BM based on individual ICD-O topography and morphology types. Furthermore, our study would help organize important clinical information and risk factors, leading to better identification, surveillance, improved patient counseling, more rigorous prognostic classification, and prophylactic treatment of cancer patients at greatest risk for BM.

## Limitations

The primary limitations of this study are its integral data quality and the retrospective design. Although all essential factors were extracted from the NCDB to mitigate the risk of confounding, the possibility of influence from unmeasured confounders cannot be excluded. Real-world data are highly complex and an incomplete reflection of reality. There is always a chance for introduction of unpredictable outliers even with basic structural data collection. In concordance with previous literature, all survival predictors were included for feature selection except for the Karnofsky Performance Scale, as no such performance status variable has been reported in the NCDB. Nevertheless, the patient performance status is indirectly reflected by the administration of radiotherapy and systemic therapy in the database, covariates for which the model was appropriately adjusted. The NCDB is a hospital-based registry, therefore the defined populations and hospitals are subject to (and limited by) the regional referral patterns, regional access to health care and cancer treatment, and the inherent sampling biases of the pathology of that region. In addition, no two regions have equivalent treatment expertise. Slight variations in clinical aggressiveness

in obtaining diagnostic imaging and/or surgery or even the frequency of biopsies potentially affect the reported incidences of BM. Randomized controlled trials would be ideal; however, it is neither practical nor feasible to establish a cohort on this scale. In addition, it is ethically unjustifiable to randomize newly diagnosed BM patients to a no-treatment placebo arm to assess for covariate significance.

## **Abbreviations**

AF, acceleration factor; AFT, accelerated failure time; AIC, Akaike information criterion; BM, brain metastases; CDscore, Charlson-Deyo comorbidity score; GI, gastrointestinal; GPA, graded prognostic assessment; HR, hazard ratio; ICD-O, International Classification of Diseases for Oncology; NCDB, National Cancer Database; NHL, Non-Hodgkin lymphoma; PH, proportional hazards; PO, proportional odds; RCC, renal cell carcinoma; SCLC small cell lung cancer.

## **Statements & Declarations**

### **Acknowledgments**

We thank the National Cancer Database which is a joint project of the American Cancer Society and the Commission on Cancer of the American College of Surgeons for providing the data used in this study. The NCDB, established in 1989, is a nationwide, facility-based, comprehensive clinical surveillance resource oncology data set that currently captures 72% of all newly diagnosed malignancies in the US annually. The American College of Surgeons and the Commission on Cancer are not responsible for the analytic or statistical methodology employed in the study. We are indebted to many clinicians for their contributions to this registry, and to the patients for participation in research.

### **Funding**

Dr. Philippe Mercier was supported by a Saint Louis University College of Medicine Clinical Research Scholarship. Statistical assistance was provided by Noor Al-Hammadi.

### **Author contributions**

Conception and design: Georgios Alexopoulos

Provision of study materials or patients: Philippe Mercier, Georgios Alexopoulos

Collection and assembly of data: Georgios Alexopoulos, Justin Zhang

Data analysis and interpretation: Georgios Alexopoulos

Manuscript writing: Georgios Alexopoulos

Assisted with manuscript writing: Justin Zhang, Mayur Patel, Ioannis Karampelas

Revised the final manuscript: Georgios Alexopoulos, Ioannis Karampelas, Philippe Mercier

Final approval of manuscript: All authors

Accountable for all aspects of the work: All authors

### Competing Interests

None declared. No potential conflict of interest related to this study is reported by the authors.

### Data Availability

*The datasets generated and analysed during the current study are available in the National Cancer Database (NCDB) repository, <https://ncdbapp.facs.org/puf/>.*

### Ethics approval

*This is an observational study. The XYZ Research Ethics Committee has confirmed that no ethical approval is required.*

## References

1. Fox BD, Cheung VJ, Patel AJ, Suki D, Rao G. Epidemiology of metastatic brain tumors. *Neurosurg Clin N Am*. 2011 Jan;22(1):1-6, v. doi: 10.1016/j.nec.2010.08.007. PMID: 21109143.
2. Nayak L, Lee EQ, Wen PY. Epidemiology of brain metastases. *Curr Oncol Rep*. 2012 Feb;14(1):48-54. doi: 10.1007/s11912-011-0203-y. PMID: 22012633.
3. Sacks P, Rahman M. Epidemiology of Brain Metastases. *Neurosurg Clin N Am*. 2020 Oct;31(4):481-488. doi: 10.1016/j.nec.2020.06.001. PMID: 32921345.
4. Ostrom QT, Wright CH, Barnholtz-Sloan JS. Brain metastases: epidemiology. *Handb Clin Neurol*. 2018;149:27-42. doi: 10.1016/B978-0-12-811161-1.00002-5. PMID: 29307358.
5. Lamba N, Wen PY, Aizer AA. Epidemiology of brain metastases and leptomeningeal disease. *Neuro Oncol*. 2021 Sep 1;23(9):1447-1456. doi: 10.1093/neuonc/noab101. PMID: 33908612; PMCID: PMC8408881.
6. Lin X, DeAngelis LM. Treatment of Brain Metastases. *J Clin Oncol*. 2015 Oct 20;33(30):3475-84. doi: 10.1200/JCO.2015.60.9503. Epub 2015 Aug 17. PMID: 26282648; PMCID: PMC5087313.
7. Lowery FJ, Yu D. Brain metastasis: Unique challenges and open opportunities. *Biochim Biophys Acta Rev Cancer*. 2017;1867(1):49-57. doi:10.1016/j.bbcan.2016.12.001
8. Valiente M, Ahluwalia MS, Boire A, et al. The Evolving Landscape of Brain Metastasis. *Trends Cancer*. 2018;4(3):176-196. doi:10.1016/j.trecan.2018.01.003
9. World Health Organization. (2013). International classification of diseases for oncology (ICD-O), 3rd ed., 1st revision. World Health Organization.

10. Cagney DN, Martin AM, Catalano PJ, Redig AJ, Lin NU, Lee EQ, Wen PY, Dunn IF, Bi WL, Weiss SE, Haas-Kogan DA, Alexander BM, Aizer AA. Incidence and prognosis of patients with brain metastases at diagnosis of systemic malignancy: a population-based study. *Neuro Oncol*. 2017 Oct 19;19(11):1511-1521. doi: 10.1093/neuonc/nox077. PMID: 28444227; PMCID: PMC5737512.
11. Gállego Pérez-Larraya J, Hildebrand J. Brain metastases. *Handb Clin Neurol*. 2014;121:1143-57. doi: 10.1016/B978-0-7020-4088-7.00077-8. PMID: 24365409.
12. Barnholtz-Sloan JS, Sloan AE, Davis FG, Vigneau FD, Lai P, Sawaya RE. Incidence proportions of brain metastases in patients diagnosed (1973 to 2001) in the Metropolitan Detroit Cancer Surveillance System. *J Clin Oncol*. 2004 Jul 15;22(14):2865-72. doi: 10.1200/JCO.2004.12.149. PMID: 15254054
13. Sperduto PW, Kased N, Roberge D, Xu Z, Shanley R, Luo X, Sneed PK, Chao ST, Weil RJ, Suh J, Bhatt A, Jensen AW, Brown PD, Shih HA, Kirkpatrick J, Gaspar LE, Fiveash JB, Chiang V, Knisely JP, Sperduto CM, Lin N, Mehta M. Summary report on the graded prognostic assessment: an accurate and facile diagnosis-specific tool to estimate survival for patients with brain metastases. *J Clin Oncol*. 2012 Feb 1;30(4):419-25. doi: 10.1200/JCO.2011.38.0527. Epub 2011 Dec 27. PMID: 22203767; PMCID: PMC3269967.
14. American College of Surgeons. National Cancer Database. <https://www-facs-org.ezp.slu.edu/quality-programs/cancer/ncdb>. Accessed March 08, 2022.
15. Gelman A, Carlin J. Beyond Power Calculations: Assessing Type S (Sign) and Type M (Magnitude) Errors. *Perspect Psychol Sci*. 2014 Nov;9(6):641-51. doi: 10.1177/1745691614551642. PMID: 26186114.
16. Alexopoulos G, Zhang J, Karampelas I, Patel M, Kemp J, Coppens J, Mattei TA, Mercier P. Long-term time series forecasting and updates on survival analysis of glioblastoma multiforme, a 1975-2018 population-based study. *Neuroepidemiology*. 2022 Feb 16. doi: 10.1159/000522611. Epub ahead of print. PMID: 35172317.
17. Athanassiou A, Begent RH, Newlands ES, Parker D, Rustin GJ, Bagshawe KD. Central nervous system metastases of choriocarcinoma. 23 years' experience at Charing Cross Hospital. *Cancer*. 1983 Nov 1;52(9):1728-35. doi: 10.1002/1097-0142(19831101)52:9<1728::aid-cnrcr2820520929>3.0.co;2-u. PMID: 6684500.
18. Sperduto PW, Chao ST, Sneed PK, Luo X, Suh J, Roberge D, Bhatt A, Jensen AW, Brown PD, Shih H, Kirkpatrick J, Schwer A, Gaspar LE, Fiveash JB, Chiang V, Knisely J, Sperduto CM, Mehta M. Diagnosis-specific prognostic factors, indexes, and treatment outcomes for patients with newly diagnosed brain metastases: a multi-institutional analysis of 4,259 patients. *Int J Radiat Oncol Biol Phys*. 2010 Jul 1;77(3):655-61. doi: 10.1016/j.ijrobp.2009.08.025. Epub 2009 Nov 26. PMID: 19942357.
19. Sperduto PW, Mesko S, Li J, Cagney D, Aizer A, Lin NU, Nesbit E, Kruser TJ, Chan J, Braunstein S, Lee J, Kirkpatrick JP, Breen W, Brown PD, Shi D, Shih HA, Soliman H, Sahgal A, Shanley R, Sperduto WA, Lou E, Everett A, Boggs DH, Masucci L, Roberge D, Remick J, Plichta K, Buatti JM, Jain S, Gaspar LE,

- Wu CC, Wang TJC, Bryant J, Chuong M, An Y, Chiang V, Nakano T, Aoyama H, Mehta MP. Survival in Patients With Brain Metastases: Summary Report on the Updated Diagnosis-Specific Graded Prognostic Assessment and Definition of the Eligibility Quotient. *J Clin Oncol*. 2020 Nov 10;38(32):3773-3784. doi: 10.1200/JCO.20.01255. Epub 2020 Sep 15. PMID: 32931399; PMCID: PMC7655019.
20. Gaspar L, Scott C, Rotman M, Asbell S, Phillips T, Wasserman T, McKenna WG, Byhardt R. Recursive partitioning analysis (RPA) of prognostic factors in three Radiation Therapy Oncology Group (RTOG) brain metastases trials. *Int J Radiat Oncol Biol Phys*. 1997 Mar 1;37(4):745-51. doi: 10.1016/s0360-3016(96)00619-0. PMID: 9128946.
21. Waqar SN, Samson PP, Robinson CG, Bradley J, Devarakonda S, Du L, Govindan R, Gao F, Puri V, Morgensztern D. Non-small-cell Lung Cancer With Brain Metastasis at Presentation. *Clin Lung Cancer*. 2018 Jul;19(4):e373-e379. doi: 10.1016/j.clcc.2018.01.007. Epub 2018 Mar 9. PMID: 29526531; PMCID: PMC6990432
22. Takayanagi A, Florence TJ, Hariri OR, Armstrong A, Yazdian P, Sumida A, Quadri SA, Cohen J, Tehrani OS. Brain metastases from cervical cancer reduce longevity independent of overall tumor burden. *Surg Neurol Int*. 2019 Sep 13;10:176. doi: 10.25259/SNI\_37\_2019. PMID: 31583173; PMCID: PMC6763668.
23. Spears WT, Morphis JG 2nd, Lester SG, Williams SD, Einhorn LH. Brain metastases and testicular tumors: long-term survival. *Int J Radiat Oncol Biol Phys*. 1992;22(1):17-22. doi: 10.1016/0360-3016(92)90977-p. PMID: 1370066.
24. Hlatky R, Suki D, Sawaya R. Carcinoid metastasis to the brain. *Cancer*. 2004 Dec 1;101(11):2605-13. doi: 10.1002/cncr.20659. PMID: 15495181.
25. Choi SY, Yoo S, You D, Jeong IG, Song C, Hong B, Hong JH, Ahn H, Kim CS. Prognostic Factors for Survival of Patients With Synchronous or Metachronous Brain Metastasis of Renal Cell Carcinoma. *Clin Genitourin Cancer*. 2017 Dec;15(6):717-723. doi: 10.1016/j.clgc.2017.05.010. Epub 2017 May 10. PMID: 28552571.
26. Ali S, Khan MT, Idrisov EA, Maqsood A, Asad-Ur-Rahman F, Abusaada K. Signet Cell in the Brain: A Case Report of Leptomeningeal Carcinomatosis as the Presenting Feature of Gastric Signet Cell Cancer. *Cureus*. 2017 Mar 7;9(3):e1085. doi: 10.7759/cureus.1085. PMID: 28405535; PMCID: PMC5384845.
27. Parasuraman S, Langston J, Rao BN, Poquette CA, Jenkins JJ, Merchant T, Cain A, Pratt CB, Pappo AS. Brain metastases in pediatric Ewing sarcoma and rhabdomyosarcoma: the St. Jude Children's Research Hospital experience. *J Pediatr Hematol Oncol*. 1999 Sep-Oct;21(5):370-7. doi: 10.1097/00043426-199909000-00007. PMID: 10524449.

## Tables

**Table 1. Frequency Tables. Incidence of Cancer Patients in the National Cancer Database (NCDB) with Synchronous Brain Metastases stratified by ICD-O Primary Topography from year 2010 to 2018.**

<b>ICD-O Primary Topography</b>	<b>Total N Cases</b>	<b>Brain Metastases at diagnosis (N,%)</b>
Anus	78,407	64 (0.08)
Biliary	108,434	225(0.21)
Bone/Joint	28,411	86 (0.30)
Breast	3,208,696	7,077 (0.22)
Cervix	148,113	317 (0.21)
Colon	1,490,531	2,814 (0.19)
Digestive tract, other	16,905	385 (2.28)
Esophagus	181,586	2,027 (1.11)
Female genitals/placenta	30,428	89 (0.29)
Gallbladder	41,967	87 (0.21)
Kidney	615,519	5,106 (0.83)
Liver	233,700	506 (0.22)
Lung, non-small cell	1,772,978	109,782 (6.19)
Lung, other	157,582	11,554 (7.33)
Lung, small cell	296,583	26,359 (8.89)
Melanoma	704,041	6,902 (0.98)
Nasal	27,600	150 (0.54)
NHL, extra-nodal	207,804	175 (0.08)
NHL, nodal	442,772	514 (0.12)
Ovary	245,465	258 (0.11)
Pancreas	459,547	1,178 (0.26)
Skin, other	47,204	56 (0.12)
Prostate	1,742,871	720 (0.04)
Small Intestine	87,435	137 (0.16)
Soft Tissues	119,330	513 (0.43)
Stomach	237,704	955 (0.40)
Testis	83,903	534 (0.64)
Trachea/Larynx/Mediastinum	150,097	130 (0.08)

Urinary Tracts	46,586	103 (0.22)
Urinary Bladder	671,462	520 (0.08)
Uterus	596,088	827 (0.14)
<b>Total Number of Patients</b>	<b>14,279,749</b>	<b>180,150(1.26)</b>

**Table 2.** Parametric Survival Analysis. Accelerated Failure Time Model Using the Best Distribution (Log-logistic) to Describe the Survival Pattern in the Population, NCDB from 2010-2018 , N = 145,429

Predictor Variable	Acceleration Factor <sup>†</sup> (95% CI)	Proportional Odds <sup>‡</sup> (95% CI)	<i>p</i> -value
<b>ICD-O topography</b>			
Prostate	*	*	*
Anus	0.32 (0.22, 0.46)	5.71 (3.26, 9.99)	<0.001
Biliary	0.25 (0.19, 0.33)	8.14 (5.37, 12.3)	<0.001
Bone/joint	0.46 (0.29, 0.72)	3.22 (1.63, 6.34)	<0.001
Breast	0.44 (0.39, 0.51)	3.44 (2.81, 4.22)	<0.001
Cervix	0.24 (0.20, 0.29)	8.68 (6.65, 11.3)	<0.001
Colon	0.32 (0.29, 0.37)	5.50 (4.55, 6.66)	<0.001
Digestive, other	0.30 (0.25, 0.35)	6.27 (4.81, 8.16)	<0.001
Esophagus	0.30 (0.26, 0.34)	6.20 (5.11, 7.53)	<0.001
Female genitals/placenta	0.31 (0.22, 0.44)	5.91 (3.49, 10.0)	<0.001
Gallbladder	0.27 (0.20, 0.36)	7.17 (4.67, 11.0)	<0.001
Kidney	0.31 (0.27, 0.36)	5.91 (4.71, 7.42)	<0.001
Liver	0.22 (0.16, 0.30)	10.1 (6.14, 16.5)	<0.001
Lung, non-small cell	0.36 (0.32, 0.40)	4.77 (3.99, 5.69)	<0.001
Lung, other type	0.31 (0.27, 0.35)	5.88 (4.83, 7.17)	<0.001
Lung, small cell	0.40 (0.33, 0.48)	4.02 (2.99, 5.40)	<0.001
Melanoma	0.29 (0.22, 0.38)	6.52 (4.28, 9.94)	<0.001
Nasal	0.39 (0.31, 0.51)	4.06 (2.77, 5.96)	<0.001

NHL Extra-nodal	0.14 (0.03, 0.58)	19.2 (2.25, 164)	0.006
NHL Nodal	0.09 (0.02, 0.39)	34.8 (4.08, 296)	0.002
Ovary	0.24 (0.19, 0.30)	8.48 (6.09, 11.8)	<0.001
Pancreas	0.26 (0.23, 0.30)	7.52 (6.12, 9.24)	<0.001
Skin, other	0.43 (0.29, 0.64)	3.62 (1.97, 6.65)	<0.001
Small Intestine	0.31 (0.24, 0.39)	5.94 (4.12, 8.57)	<0.001
Soft Tissues	0.34 (0.27, 0.43)	5.10 (3.61, 7.21)	<0.001
Stomach	0.27 (0.24, 0.31)	7.20 (5.81, 8.93)	<0.001
Testis	0.46 (0.29, 0.72)	3.27 (1.65, 6.45)	<0.001
Trachea/Larynx/Mediastinum	0.38 (0.27, 0.53)	4.35 (2.58, 7.34)	<0.001
Urinary Tracts	0.28 (0.21, 0.39)	6.58 (4.20, 10.3)	<0.001
Urinary Bladder	0.29 (0.24, 0.36)	6.44 (4.77, 8.71)	<0.001
Uterus	0.24 (0.21, 0.29)	8.49 (6.61, 10.9)	<0.001
<b>Facility Type</b>			
Academic/Research Program	1.06 (1.01, 1.12)	0.91 (0.84, 0.99)	0.035
Community Cancer Program	0.90 (0.85, 0.95)	1.17 (1.07, 1.29)	<0.001
Comprehensive Community Cancer Program	0.92 (0.87, 0.97)	1.14 (1.05, 1.24)	0.003
Integrated Cancer Program	0.92(0.87, 0.98)	1.13 (1.03, 1.23)	0.007
<b>Age</b>	0.99 (0.988, 0.989)	1.02 (1.02, 1.02)	<0.001
<b>Sex—Male</b>	0.87 (0.855, 0.877)	1.24 (1.22, 1.27)	<0.001
<b>Race</b>			

Black	*	*	*
American Indian or Eskimo	0.89 (0.80, 0.99)	1.18 (1.01, 1.39)	0.041
Asian	1.30 (1.25, 1.36)	0.67 (0.63, 0.72)	<0.001
Other	1.22 (1.13, 1.32)	0.74 (0.66, 0.83)	<0.001
Pacific Islander	1.16 (1.01, 1.34)	0.79 (0.64, 0.98)	0.036
Unknown	1.12 (1.04, 1.21)	0.84 (0.75, 0.94)	0.002
White	0.92 (0.90, 0.94)	1.13 (1.10, 1.16)	<0.001
<b>Median Income (2016)</b>			
\$30,000 to 34,999	0.96 (0.85, 1.10)	1.06 (0.87, 1.28)	0.580
\$35,000 to 45,999	0.99 (0.87, 1.13)	1.02 (0.83, 1.24)	0.877
Above \$46,000	1.08 (0.95, 1.23)	0.89 (0.73, 1.08)	0.227
Less \$30,000	0.92 (0.81, 1.05)	1.13 (0.93, 1.38)	0.214
<b>Urban or Rural (2013)</b>			
Metropolitan	0.95 (0.91, 0.98)	1.09 (1.02, 1.15)	0.006
Rural	0.91 (0.86, 0.97)	1.15 (1.05, 1.25)	0.002
Urban	0.93 (0.89, 0.97)	1.12 (1.05, 1.19)	<0.001
<b>High school degree (2016)</b>			
10.9% to 17.6%	0.97 (0.84, 1.12)	1.05 (0.85, 1.31)	0.647
6.3% to 10.8%	0.95 (0.82, 1.10)	1.08 (0.87, 1.34)	0.497
Above 17.6%	1.03 (0.89, 1.19)	0.95 (0.77, 1.18)	0.662
Less 6.3%	0.97 (0.84, 1.11)	1.05 (0.85, 1.31)	0.640

## Total Charlson-Deyo Score

0	*	*	*
1	0.87 (0.85, 0.88)	1.24 (1.22, 1.27)	<0.001
2	0.80 (0.79, 0.82)	1.38 (1.34, 1.43)	<0.001
3	0.76 (0.74, 0.78)	1.52 (1.45, 1.59)	<0.001
<b>Great Circle Distance (miles)</b>	1 (1, 1)	1 (1, 1)	<0.001
<b>ICD-O morphology</b>			
Choriocarcinoma, NOS	*	*	*
Acinar cell carcinoma	0.39 (0.22, 0.68)	4.23 (1.81, 9.88)	<0.001
Acinar cell cystadenocarcinoma	0.15 (0.02, 1.00)	18.1 (0.99, 328)	0.050
Adenocarcinomas, other	0.27 (0.15, 0.46)	7.44 (3.24, 17.1)	<0.001
Adenosquamous carcinoma	0.22 (0.13, 0.38)	9.95 (4.31, 23.0)	<0.001
Adnexal and skin appendage neoplasms	0.19 (0.09, 0.42)	12.0 (3.74, 38.7)	<0.001
Atypical carcinoid tumor	0.35 (0.19, 0.65)	4.83 (1.91, 12.2)	<0.001
Basal cell carcinomas, other	0.11 (0.02, 0.75)	27.7 (1.53, 501)	0.024
Basaloid squamous cell carcinoma	0.24 (0.13, 0.43)	8.67 (3.50, 21.5)	<0.001
Blood vessel tumors, other	0.45 (0.17, 1.17)	3.34 (0.78, 14.2)	0.103
Carcinoid tumor, NOS	0.52 (0.28, 0.93)	2.72 (1.11, 6.68)	0.029
Carcinoma, other	0.21 (0.12, 0.36)	10.9 (4.74, 25.1)	<0.001
Carcinoma, undifferentiated, NOS	0.17 (0.09, 0.31)	14.6 (5.88, 36.4)	<0.001
Carcinosarcoma, NOS	0.22 (0.12, 0.40)	9.82 (4.02, 24.0)	<0.001
Cholangiocarcinoma	0.27 (0.15, 0.51)	7.17 (2.80, 18.4)	<0.001

Clear cell adenocarcinoma, NOS	0.33 (0.19, 0.57)	5.46 (2.34, 12.7)	<0.001
CNS embryonal tumor, NOS	0.10 (0.02, 0.42)	32.6 (3.71, 287)	0.002
Combined small cell carcinoma	0.21 (0.12, 0.38)	10.6 (4.39, 25.7)	<0.001
Complex epithelial neoplasms	0.19 (0.09, 0.37)	12.3 (4.51, 33.8)	<0.001
Complex mixed and stromal neoplasms	0.19 (0.10, 0.35)	12.7 (4.90, 33.0)	<0.001
Cystic, mucinous, and serous carcinomas	0.53 (0.26, 1.07)	2.61 (0.90, 7.53)	0.076
Ductal and lobular carcinomas, other	0.24 (0.12, 0.45)	8.77 (3.33, 23.1)	<0.001
Endometrioid adenocarcinoma, NOS	0.23 (0.13, 0.41)	9.21 (3.84, 22.1)	<0.001
Ewing sarcoma	0.17 (0.08, 0.37)	14.0 (4.55, 43.3)	<0.001
Fibroepithelial neoplasms	0.08 (0.02, 0.29)	42.7 (6.42, 284)	<0.001
Fibromatous neoplasms	0.22 (0.11, 0.43)	10.2 (3.57, 28.9)	<0.001
Germ cell neoplasms	0.07 (0.02, 0.20)	56.0 (11.8, 267)	<0.001
Giant cell tumors	0.12 (0.02, 0.53)	24.7 (2.64, 231)	0.005
Granular cell tumors and alveolar soft part sarcomas	0.71 (0.32, 1.56)	1.69 (0.51, 5.57)	0.390
Hemangiosarcoma	0.14 (0.08, 0.27)	18.6 (7.30, 47.2)	<0.001
Hepatocellular carcinoma, all types	0.26 (0.14, 0.50)	7.53 (2.86, 19.8)	<0.001
Hepatoid adenocarcinoma	0.19 (0.09, 0.38)	11.7 (4.21, 32.8)	<0.001
Infiltrating duct and lobular carcinoma	0.29 (0.16, 0.53)	6.42 (2.64, 15.6)	<0.001
Infiltrating duct carcinoma, NOS	0.24 (0.13, 0.41)	8.93 (3.86, 20.7)	<0.001
Infiltrating duct mixed with other types of carcinoma	0.31 (0.17, 0.58)	5.78 (2.26, 14.8)	<0.001
Inflammatory carcinoma	0.19 (0.10, 0.34)	12.7 (5.10, 31.4)	<0.001

Large cell carcinoma, NOS	0.21 (0.12, 0.36)	10.8 (4.66, 24.9)	<0.001
Large cell neuroendocrine carcinoma	0.23 (0.13, 0.41)	8.96 (3.88, 20.7)	<0.001
Leiomyosarcoma, NOS	0.27 (0.14, 0.50)	7.25 (2.87, 18.3)	<0.001
Lepidic adenocarcinoma	0.32 (0.18, 0.57)	5.57 (2.35, 13.2)	<0.001
Leukemias, other	2.70 (0.56, 13.0)	0.22 (0.02, 2.40)	0.216
Lipomatous sarcomas	0.25 (0.11, 0.53)	8.38 (2.62, 26.8)	<0.001
Lobular carcinoma, NOS	0.25 (0.14, 0.44)	8.32 (3.52, 19.6)	<0.001
Lymphoid leukemias	0.82 (0.17, 4.0)	1.35 (0.12, 14.8)	0.808
Malignant lymphoma, diffuse	1.41 (0.32, 6.15)	0.59 (0.06, 5.51)	0.646
Malignant lymphoma, large B-cell, diffuse, NOS	0.84 (0.22, 3.09)	1.31 (0.18, 9.44)	0.790
Malignant lymphoma, non-Hodgkin, NOS	1.33 (0.33, 5.31)	0.65 (0.08, 5.23)	0.683
Malignant melanoma, NOS	0.38 (0.21, 0.69)	4.33 (1.74, 10.8)	0.002
Malignant peripheral nerve sheath tumor	0.19 (0.09, 0.40)	12.7 (3.99, 40.4)	<0.001
Malignant tumor, NOS	0.31 (0.15, 0.64)	5.82 (1.96, 17.3)	0.002
Mature B-cell lymphomas, other	2.10 (0.55, 8.07)	0.32 (0.04, 2.49)	0.279
Mature T- and NK-cell lymphomas	0.63 (0.16, 2.51)	2.03 (0.25, 16.7)	0.508
Melanoma, other	0.38 (0.20, 0.71)	4.38 (1.70, 11.3)	0.002
Miscellaneous tumors, other	0.47 (0.07, 3.15)	3.15 (0.18, 56.5)	0.436
Mixed cell adenocarcinoma	0.32 (0.17, 0.60)	5.56 (2.16, 14.4)	<0.001
Mucin-producing adenocarcinoma	0.26 (0.15, 0.46)	7.53 (3.17, 17.9)	<0.001

Mucinous adenocarcinoma	0.24 (0.14, 0.41)	8.75 (3.78, 20.3)	<0.001
Mucoepidermoid carcinoma	0.26 (0.12, 0.59)	7.47 (2.19, 25.5)	0.001
Mullerian mixed tumor	0.23 (0.11, 0.48)	9.03 (3.08, 26.5)	<0.001
Myomatous neoplasms, other	0.15 (0.07, 0.29)	17.8 (6.31, 50.0)	<0.001
Myxomatous neoplasms	2.20 (0.41, 11.9)	0.30 (0.02, 3.91)	0.360
Neoplasm, malignant	0.16 (0.09, 0.28)	15.9 (6.91, 36.7)	<0.001
Neuroendocrine carcinoma, NOS	0.24 (0.14, 0.43)	8.39 (3.64, 19.3)	<0.001
Neuroepitheliomatous neoplasms	0.78 (0.30, 2.09)	1.45 (0.33, 6.44)	0.624
Nodular melanoma	0.25 (0.14, 0.47)	7.95 (3.11, 20.3)	<0.001
Non-small cell carcinoma	0.21 (0.12, 0.36)	10.6 (4.60, 24.3)	<0.001
Oat cell carcinoma	0.20 (0.11, 0.38)	11.1 (4.35, 28.1)	<0.001
Osseous and chondromatous neoplasms	0.14 (0.07, 0.29)	19.5 (6.34, 59.7)	<0.001
Papillary adenocarcinoma, NOS	0.39 (0.22, 0.68)	4.12 (1.77, 9.58)	<0.001
Papillary carcinoma, NOS	0.25 (0.13, 0.47)	8.14 (3.10, 21.4)	<0.001
Papillary transitional cell carcinoma	0.26 (0.14, 0.49)	7.53 (2.97, 19.1)	<0.001
Paragangliomas and glomus tumors	3.56 (0.52, 24.3)	0.15 (0.01, 2.68)	0.195
Plasma cell tumors	1 (1, 1)	1 (1, 1)	N/A
Pleomorphic carcinoma	0.19 (0.10, 0.34)	12.7 (5.19, 30.9)	<0.001
Pseudosarcomatous carcinoma	0.18 (0.10, 0.31)	13.8 (5.92, 32.2)	<0.001
Renal cell carcinoma, NOS	0.27 (0.15, 0.47)	7.19 (3.08, 16.8)	<0.001

Renal cell carcinoma, other	0.23 (0.10, 0.50)	9.26 (2.83, 30.3)	<0.001
Renal cell carcinoma, sarcomatoid	0.17 (0.09, 0.31)	14.0 (5.81, 33.9)	<0.001
Serous carcinoma, NOS	0.29 (0.16, 0.55)	6.34 (2.46, 16.3)	<0.001
Signet ring cell carcinoma	0.19 (0.11, 0.34)	12.2 (5.22, 28.6)	<0.001
Small cell carcinoma, intermediate cell	0.21 (0.10, 0.42)	10.8 (3.75, 31.0)	<0.001
Small cell carcinoma, NOS	0.20 (0.11, 0.36)	11.1 (4.68, 26.5)	<0.001
Soft tissue sarcomas, NOS	0.18 (0.10, 0.33)	12.8 (5.30, 31.1)	<0.001
Solid carcinoma, NOS	0.30 (0.16, 0.55)	6.15 (2.47, 15.3)	<0.001
Specialized gonadal neoplasms	0.07 (0.01, 0.49)	53.2 (2.90, 975)	0.007
Spindle cell carcinoma, NOS	0.14 (0.07, 0.26)	19.4 (7.77, 48.4)	<0.001
Spindle cell melanoma, NOS	0.43 (0.21, 0.86)	3.61 (1.25, 10.4)	0.018
Spindle cell sarcoma	0.17 (0.09, 0.33)	14.5 (5.34, 39.2)	<0.001
Squamous cell carcinoma, keratinizing, NOS	0.20 (0.12, 0.36)	10.7 (4.61, 25.0)	<0.001
Squamous cell carcinoma, large cell, non-keratinizing, NOS	0.22 (0.13, 0.39)	9.72 (4.12, 23.0)	<0.001
Squamous cell carcinoma, NOS	0.21 (0.12, 0.36)	10.6 (4.62, 24.4)	<0.001
Squamous cell carcinoma, spindle cell	0.18 (0.09, 0.34)	13.5 (4.97, 36.5)	<0.001
Squamous cell neoplasms, other	0.18 (0.09, 0.36)	13.1 (4.71, 36.3)	<0.001
Struma ovarii, malignant	0.20 (0.10, 0.38)	11.6 (4.35, 30.8)	<0.001
Synovial sarcomas	0.16 (0.08, 0.34)	15.5 (5.10, 47.3)	<0.001
Thymic epithelial neoplasms	0.14 (0.02, 0.98)	18.5 (1.03, 335)	0.048

Transitional cell carcinomas, other	0.23 (0.13, 0.41)	9.09 (3.83, 21.6)	<0.001
Trophoblastic neoplasms, other	0.53 (0.15, 1.87)	2.56 (0.39, 16.9)	0.329
<b>Summary of Surgical Margins (surgery at primary site)</b>			
Macroscopic residual tumor	*	*	*
Margins not evaluable	0.97 (0.79, 1.19)	1.04 (0.76, 1.41)	0.800
Microscopic residual tumor	1.31 (1.06, 1.62)	0.66 (0.48, 0.91)	0.011
No primary site surgery	0.84 (0.67, 1.0)	1.31 (0.99, 1.72)	0.053
No residual tumor	2.07 (1.72, 2.49)	0.33 (0.25, 0.44)	<0.001
Residual tumor, NOS	1.13 (0.93, 1.38)	0.83 (0.61, 1.12)	0.218
Unknown	1.38 (1.14, 1.68)	0.61 (0.46, 0.82)	0.001
<b>Summary of Chemotherapy</b>			
Administered	*	*	*
Contraindicated	0.30 (0.29, 0.30)	6.30 (6.03, 6.59)	<0.001
Not administered	0.38 (0.37, 0.39)	4.31 (4.13, 4.49)	<0.001
Not administered, patient died	0.18 (0.18, 0.19)	12.6 (12.0, 13.2)	<0.001
Not part of first course Tx	0.35 (0.35, 0.36)	4.84 (4.73, 4.95)	<0.001
Unknown	0.63 (0.61, 0.66)	2.0 (1.88, 2.13)	<0.001
<b>Summary of Radiation Therapy</b>			
Administered	*	*	*
Contraindicated	0.54 (0.51, 0.57)	2.52 (2.31, 2.76)	<0.001
Not administered	0.74 (0.71, 0.76)	1.59 (1.50, 1.68)	<0.001
Not administered, patient died	0.37 (0.32, 0.44)	4.45 (3.49, 5.68)	<0.001

Not part of first course Tx	0.71 (0.69, 0.71)	1.69 (1.65, 1.73)	<0.001
Unknown	0.71 (0.68, 0.73)	1.69 (1.60, 1.79)	<0.001
<b>Summary of Immunotherapy</b>			
Administered	*	*	*
Contraindicated	0.51 (0.45, 0.58)	2.78 (2.30, 3.35)	<0.001
Not administered	0.63 (0.55, 0.72)	2.01 (1.66, 2.44)	<0.001
Not administered, patient died	0.37 (0.32, 0.43)	4.43 (3.59, 5.47)	<0.001
Not part of first course Tx	0.49 (0.48, 0.51)	2.89 (2.78, 3.01)	<0.001
Unknown	0.82 (0.71, 0.93)	1.36 (1.12, 1.65)	0.002
<b>Summary of Hormone Therapy</b>			
Administered	*	*	*
Contraindicated	0.56 (0.52, 0.59)	2.43 (2.18, 2.70)	<0.001
Not administered	0.54 (0.51, 0.57)	2.53 (2.34, 2.74)	<0.001
Not administered, patient died	0.27 (0.22, 0.32)	7.39 (5.58, 9.80)	<0.001
Not part of first course Tx	0.66 (0.63, 0.69)	1.88 (1.76, 2.0)	<0.001
Unknown	0.54 (0.50, 0.57)	2.55 (2.32, 2.81)	<0.001
<b>Coexisting liver metastasis at diagnosis</b>			
No	*	*	*
Not applicable	0.86 (0.61, 1.22)	1.26 (0.74, 2.13)	0.398
Unknown	0.85 (0.81, 0.89)	1.28 (1.20, 1.38)	<0.001
Yes	0.63 (0.62, 0.64)	1.99 (1.95, 2.04)	<0.001

Abbreviations: NHL, non-Hodgkin lymphoma; NOS, not otherwise specified; Tx, treatment.

\*Reference group for each respective explanatory variable in the multiple regression model. Whenever a reference category is not specified, the coefficients of the explanatory are compared to either blank values or the excluded group for binary variables (e.g., the reference group for variable “Sex” is “female”).

†The acceleration factor or AF in a log-logistic model is interpretable as multiplicative effects on the survival. This suggests that the median life expectancy of each corresponding group is AF times that of the reference group for the respective explanatory.

‡ The proportional odds or PO in a log-logistic model is interpretable as multiplicative effects on the hazard, likewise semiparametric Hazard Ratios. This suggests that the odds of death or hazard for each group is PO times the odds of the reference group for the respective explanatory in the model.

## Figures

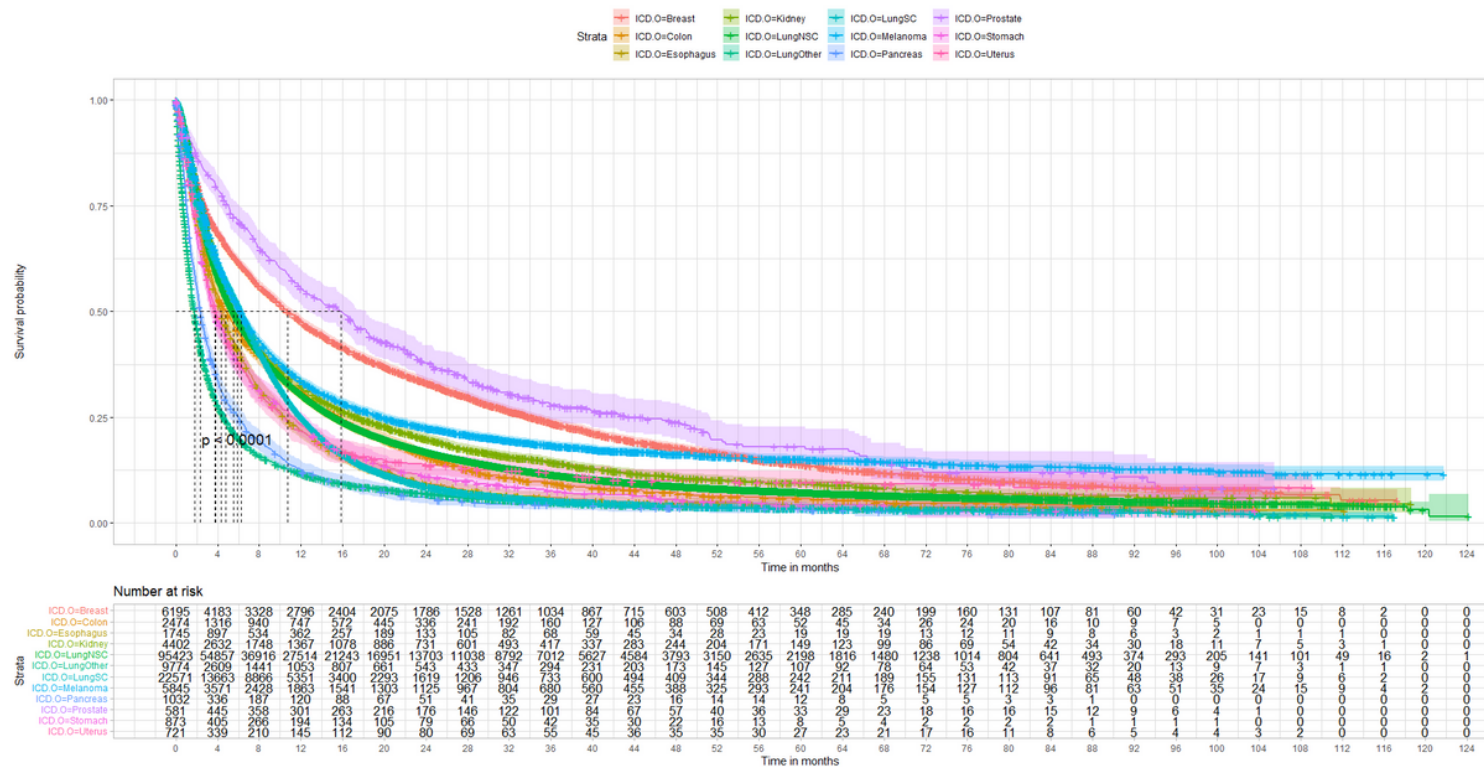
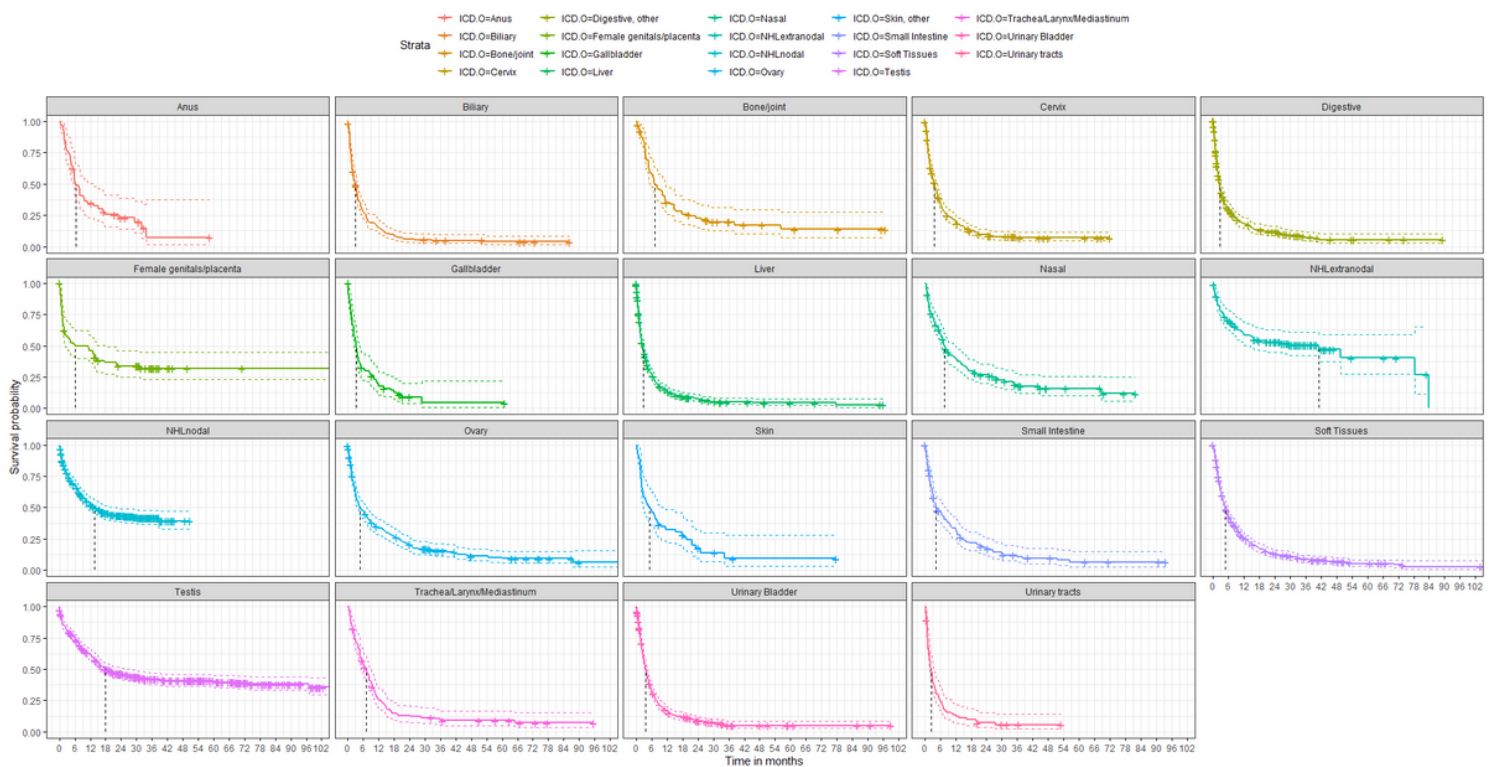


Figure 1

Kaplan-Meier survival estimates of NCD B patients presenting with brain metastases (BM) at diagnosis of systemic malignancy stratified by most frequent ICD-O primary topography types. The horizontal axis (x-axis) represents time in months following the diagnosis of systemic malignancy, and the vertical axis (y-axis) shows the survival probability. The colored lines represent survival curves of twelve distinct primary topography types along with the respective 95% confidence intervals in colored dashed lines. The number of patients at risk per primary topography immediately before timepoints (t) divided in 4-month intervals is shown in the lower part of the survival plot. Patients at risk did not have the event before time t, and are

not censored before or at time  $t$ . The  $p$ -value of the Log-Rank test comparing the twelve topography groups is also demonstrated ( $p < 0.0001$ ). The topography prostate provided the strongest overall survival benefit among most frequent sites of origin, as patients with BM from prostate cancer had a 14-month median overall increase in the survival probability. Patients with breast cancer had a survival probability,  $S(t)$ , of 10.7 months (95%CI[10.2,11.5]). This was followed by melanoma,  $S(t) = 6.24$  months (95%CI[5.98,6.57]) and small cell lung cancer,  $S(t) = 6.24$  months (95%CI[6.14,6.37]). BM from lung cancer/other type,  $S(t) = 1.8$  months (95%CI[1.74,1.84]) and pancreas,  $S(t) = 2.3$  months (95%CI[2.20,2.60]) had the lowest median survival rates among most frequent topography types.



**Figure 2**

**Matrix of Kaplan-Meier survival estimates of NCD B patients presenting with brain metastases (BM) at diagnosis of systemic malignancy stratified by least frequent ICD-O primary topography types.** The horizontal axis (x-axis) represents time in months following the diagnosis of systemic malignancy, and the vertical axis (y-axis) shows the survival probability. The colored lines represent survival curves of nineteen distinct primary topography types along with the respective 95% confidence intervals in colored dashed lines. The vertical black dotted lines demonstrate the medial survival times for the respective topography types. The topography testicular cancer provided the strongest survival benefit among least frequent sites of BM origin,  $S(t) = 17.9$  months (95%CI[15.2,26.9];  $p < 0.0001$ ) and the highest median survival in the study. Patients with nodal NHL had a  $S(t)$  of 13.6 months (95%CI[10.6,20.3];  $p < 0.0001$ ). BM from liver  $S(t) = 2.56$  months (95%CI[2.10,3.06];  $p < 0.0001$ ), urinary tracts,  $S(t) = 2.4$  months (95%CI[1.87,3.30];  $p < 0.0001$ ) and the GI tract,  $S(t) = 2.53$  months (95%CI[2.20,2.96];  $p < 0.0001$ ) had the

poorest survival rates among least frequent topography types. NHLnodal, nodal non-Hodgkin lymphoma; NHLExtr, extra-nodal non-Hodgkin lymphoma.

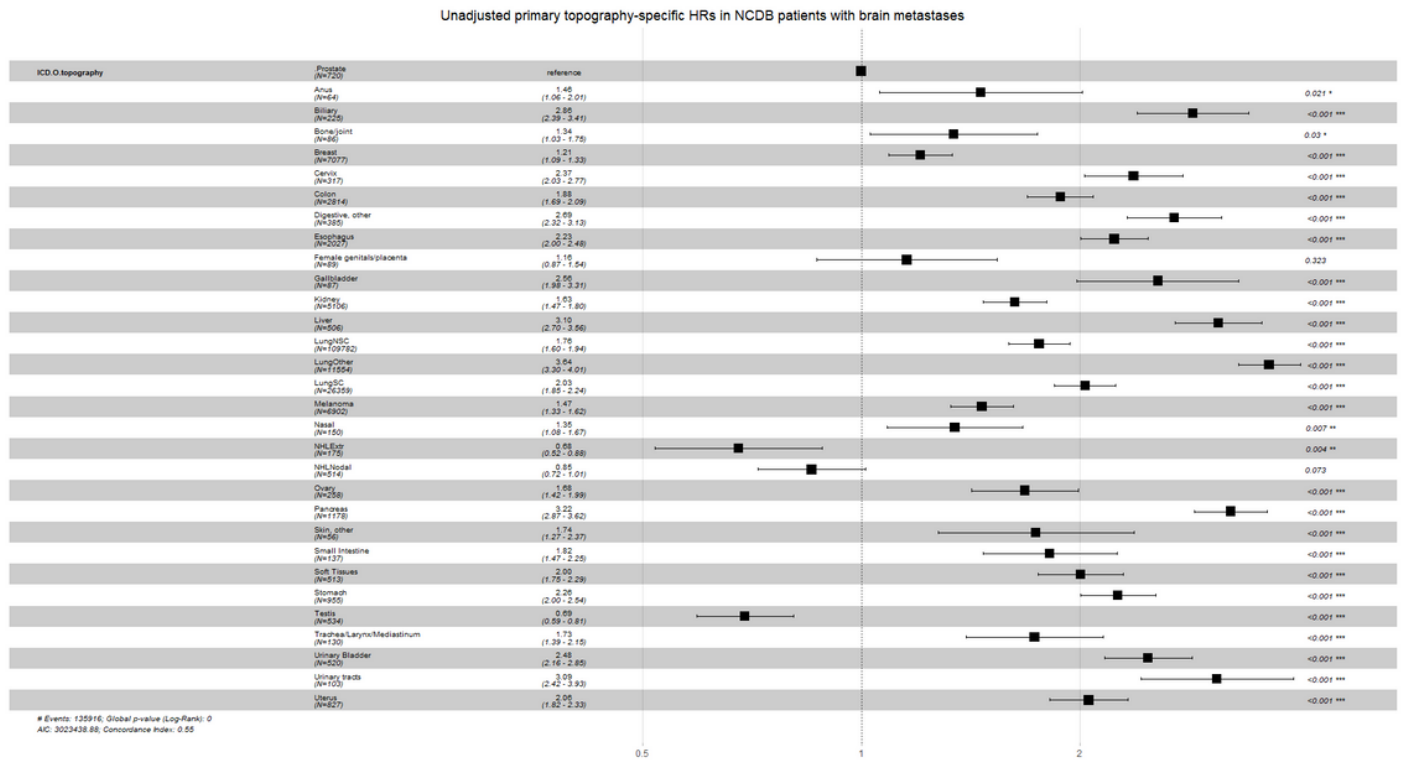


Figure 3

**Forest plot for univariate Cox proportional hazards model.** The hazard ratios (HRs) for each respective ICD-O primary topography in cancer patients with brain metastases (BM) are demonstrated. The HRs are interpretable as multiplicative effects on the hazard. Prostate cancer was set as the reference group in the model. BM from liver cancer (HR= 3.10, 95%CI[2.70,3.56]) and pancreas (HR= 3.22, 95%CI[2.87,3.61]) are strongly associated with poor patient survival. The primary topography types including pancreas, liver, biliary tree, and urinary tracts are bad prognostics, while lung (other type) demonstrates the highest hazard (HR= 3.64, 95%CI[3.30,4.01]). Testicular cancer and extra-nodal NHL are good prognostics, when compared to BM from prostate cancer. Unfortunately, frank violations of the PH assumption for multiple covariates in Cox regression make the models unable to generalize (Schoenfeld residuals: p-value < 0.0001).

Focused parametric model comparison

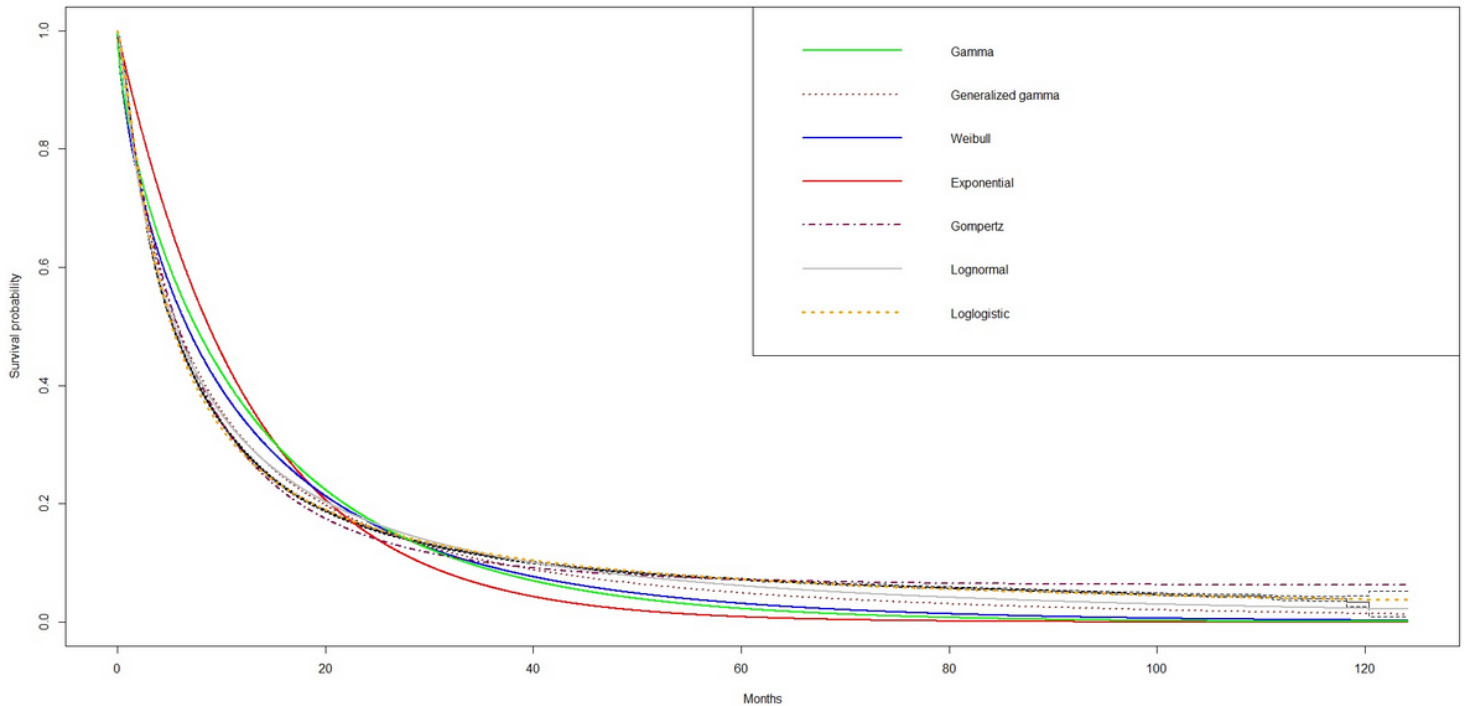


Figure 4

**Focused parametric model comparison.** Model goodness of fit tests by graphical comparison between parametric and non-parametric regression. Overplotting estimations from non-parametric Kaplan-Meier estimator (black line) versus parametric estimations utilizing exponential (red line), Weibull (blue line), Gompertz (dot-dashed pink line), gamma (green line), generalized gamma (dotted brown line), lognormal (grey line) and log-logistic (dotted orange line) distributions to identify the best survival population pattern to describe the dataset. The loglogistic distribution best fits to the non-parametric survival function as shown in the image; the distribution also achieved the lowest AIC = 915163 and Log-likelihood = -457577 among models. Therefore, a log-logistic accelerated failure model can explain the greatest amount of variation in the NCDDB population using the fewest possible information. Note that the non-parametric model is closer to the observed data because no function is assumed for the baseline survival probability.

## Supplementary Files

This is a list of supplementary files associated with this preprint. Click to download.

- [Tablesupplemental.docx](#)